Available online at www.sciencedirect.com
SCIENCE DIRECT
Electrochimica Acta 51 (2006) 4291–4301
ELECTROCHIMICA Acta
www.elsevier.com/locate/electacta

Electrodeposited Prussian blue films: Annealing effect

S.A. Agnihotry *, Punita Singh, Amish G. Joshi, D.P. Singh, K.N. Sood, S.M. Shivaprasad

National Physical Laboratory, Dr. K.S. Krishnan Road, New Delhi 110012, India

Received 10 August 2005; received in revised form 9 December 2005; accepted 10 December 2005
Available online 19 January 2006

Abstract

The correlation between the temperature-dependent electrochromic (EC) activity and other properties of galvanostatically deposited Prussian Blue (PB) films is presented here. Films subjected to annealing treatment in air at temperatures up to 500 °C were characterized by a variety of techniques which include TGA, XRD, FTIR, UV–vis spectrophotometry, SEM, XPS, cyclic voltammetry etc. The as-deposited X-ray amorphous hydrated PB films were blue in color and had Fe in both Fe^{II} and Fe^{III} valence states and were electrochromically active. Consequent to changes in the valence state, degree of hydration and coordination environment of the iron ions upon annealing, EC activity and morphology of the films exhibited dramatic changes. Annealing at moderate temperatures retained the blue color of the films and decreased the EC activity consistent with dehydration and decreased the Fe^{II} content. Lack of EC activity at higher temperatures was consistent with dehydration and quenching of Fe^{II} states accompanied with change of color from blue to rust (Fe^{III}) typical of Fe_2O_3. Independent of the annealing temperature, the films retained their amorphicity, however, prolonged annealing at 500 °C yielded hexagonal Fe_2O_3.

PACS: 81.15.Lm; 81.40Tv; 68.55.No

Keywords: Prussian blue; Electrochromic; Annealing effect; Iron hexacyanoferrate; Fe_2O_3

1. Introduction

Electrochromic (EC) devices can be used for various architectural and non-architectural applications. Architectural applications include energy efficient glazings, privacy glasses, skylights etc. Automotive glazings including sunroofs and mirrors are also important applications. The worldwide effort to develop EC devices has increased rapidly in recent years and the process of commercialization of EC devices like EC windows (ECWs) is on [1–3]. A variety of electrochromic technologies and media have been developed.

Electrochromic tungsten trioxide (WO_3) films prepared by various techniques have been investigated extensively and the potential of these films as primary electrochromic electrodes in ECWs has been established. A truly stable ECW would need an electrochemically reversible counter electrode in conjunction with WO_3 electrode and the best choice would be that of a complimentary type: coloring and bleaching in phase with WO_3, i.e., an anodically coloring and cathodically bleaching counter electrode. Enhanced radiation modulation is possible with such a configuration. Prussian blue (PB) a candidate with such properties has an additional advantage in that its color in the oxidized state is also blue, similar to that of WO_3 in the reduced state. Most importantly PB is inexpensive and can be very easily electrodeposited on conducting and semiconducting substrates. Freshly deposited blue PB films have been shown to be highly hydrated [4].

In the past, various attempts have been made to assemble electrochromic devices (ECDs) based on WO_3 and PB with different electrolytes either in the laminated or other suitable form mainly decided by the nature of the electrolyte. Generally as-deposited PB films that are microcrystalline or amorphous, are used without any further annealing treatment. Habib et al. [5] reported an ECD with a polymer electrolyte based on polyvinyl alcohol doped with H_3PO_4 and KH_2PO_4 sandwiched between the two electrodes. The spectral characteristics of the colored device confirmed the complimentary coloration of the device with coloration efficiencies of 127.7 and 138 cm^2/C, respectively at 690 and 850 nm. Laminated complimentary devices

* Corresponding author. Tel.: +91 11 25742610/91 11 2574 2610x2283; fax: +91 11 2572 6938 6952.
E-mail address: agni@mail.nplindia.ernet.in (S.A. Agnihotry).

0013-4686/$ – see front matter © 2005 Elsevier Ltd. All rights reserved.
doi:10.1016/j.electacta.2005.12.008

have also been reported by Ho et al. [6–8]. All solid state ECWs employing a poly(ethylene oxide) gel electrolyte cast onto the WO_3 film and pressed together with a PB counter electrode and edges sealed with epoxy after three days of gelation were fabricated by Su et al. [9]. However, all such attempts were mainly for EC devices on the laboratory scale and were restricted to small area ECDs. Large area electrochromic glazing with ion-conducting polyvinyl butyral (PVB) reported recently by Heckner and Kraft [10] exhibited coloration efficiency value of about 150 cm^2/C in the visible region.The ion conducting PVB layer in these devices was laminated between the two electrodes.

Durability – a technically very important parameter of ECDs depends mainly on the fabrication concepts and is one of the factors that has been responsible for not allowing ECWs to enter the market place. Attempts are continuously on for enhancing the durability of ECWs. One such step in this direction is the use of in situ polymerization of the electrolytes. However, these devices include electrically non-conductive gasket, which forms a seal with the two electrodes. The choice of the gasket material depends on factors like chemical stability to the electrolyte, impermeability to water and atmosphere and robustness over a wide temperature range. Perfect sealing of the gasket prior to electrolyte filling is of prime importance and for some of the gasket materials fulfilling the desired properties, sealing requires annealing at moderate temperatures, e.g., 80–100 °C. Systematic investigations are thus necessary to explore the effect of annealing on electrochromic and other properties of electrodeposited PB films which, otherwise are used without any annealing treatment. With this as the main objective, PB films were subjected to annealing treatment at moderate temperature (100 °C). The annealing treatment was further extended in steps to higher temperatures up to 500 °C to examine the effect of complete dehydration of the films likely to take place at intermediate temperatures and to identify the phase, no more blue but rust in color, formed at higher temperatures and to understand the mechanism of its evolution.

As-deposited and annealed PB films were thus investigated for their electrochromic performance and were characterized using a variety of techniques such as scanning electron microscopy (SEM), X-ray diffraction (XRD), X-ray photoelectron spectroscopy (XPS), FTIR spectroscopy, UV–vis spectrophotometry, cyclic voltammetry (CV). The details of the results of these investigations and their interrelation are presented in this paper.

2. Experimental

2.1. Deposition of PB films

The PB films were deposited galvanostatically on transparent conducting coated (SnO_2:F-FTO) glass plates with a current density of 10 $\mu A/cm^2$ using equivolume mixture of 10 mM $FeCl_3$ and 10 mM $K_3Fe(CN)_6$ in 0.01 N HCl (pH 2). The counter electrode used was a platinum sheet of area comparable with that of the substrate. The PB films of different thickness could be obtained by controlling the time of electrodeposition, e.g., the deposition time of 10–15 min yielded PB films with the thickness in the range 1800–2600 Å.

2.2. Characterization techniques

2.2.1. Thermal characterization

To carry out thermal studies powdered PB sample was obtained by scraping the film from the substrate. Such powdered sample was subjected to differential scanning calorimetry (DSC) and thermogravimetric analysis (TGA) between room temperature (RT) and 520 °C at a heating rate of 10 °C/min in a nitrogen atmosphere.

2.2.2. Morphological, structural, compositional & optical characterization

The PB films were annealed in air at temperatures 100, 220, 350, and 500 °C each for 15 min allowing them to cool slowly to room temperature. The surface morphological characteristics of all the films were examined and the EDX analysis was carried out using Leo 440 scanning electron microscope (SEM) which offered a resolution of 5.5 nm. XRD patterns of the films were recorded in the 2θ range from 3° to 70° with a D8 Advance Brucker Diffractometer, the wavelength of the Cu Kα radiation being 1.5418 Å. XPS characterization was carried out using Perkin-Elmer model 1257 working at a base pressure of 5×10^{-5} Torr with dual anode MgKα/AlKα 1253.6 eV X-ray source and hemispherical sector analyzer capable of 25 meV resolution. Transmission spectra of the films were recorded in the bleached as well as colored state in the range 300–800 nm with respect to air, in a UV-3101 PC Shimadzu spectrophotometer. FTIR spectra were recorded in reflection mode with respect to air using Perkin-Elmer GX 2000 OPTICA spectrophotometer in the range 4000–400 cm^{-1}.

2.2.3. Electrochromic characterization

The electrochromic performance evaluation of the films was carried out by multiple step chronoamperometry using an automated set-up comprising a He–Ne laser source ($\lambda = 632.8$ nm) and a Si photodetector sensor and a custom made microprocessor controlled versatile unit hooked on to a computer. The PB films were illuminated with the He–Ne laser beam and the photodiode was used to sense the light intensity transmitted through the film. The unit supplied a square wave potential of amplitude ± 1 V with a frequency of 0.0016 Hz for activating the electrochromic electrode in an electrolyte solution of lithium perchlorate in propylene carbonate of one molar strength (1 M $LiClO_4$-PC). A platinum counter electrode in conjunction with the PB film was used for these investigations. Plots of sensor output (percentage transmission in arbitrary units) and current flowing in the working electrode as a function of time yielded response times and ion storage capacities of the PB films, respectively. In this report, coloration time t_c is defined as the time required for the transmission of the film to decrease from 90 to 10% in the coloration cycle and bleaching time t_b is defined as the time taken for the transmission to increase from 10 to 90% in the bleaching cycle. Cyclic voltammetry for the films was performed in a classical three-electrode electrochemical cell between −1 and +1 V

wherein a PB film deposited on FTO coated glass substrate acted as the working electrode. Ag/AgCl/KCl and a Pt were employed respectively as the reference and the auxiliary electrode. The measurements were performed after cycling the film 10 times at 20 mV/s in a liquid electrolyte (1 M $LiClO_4$-PC) in an inert nitrogen atmosphere with an Omni 90 Potentiostat, Cypress Systems Inc. USA. Such a repetitive cycling endowed reversibility to the subsequent switchings between the colored and bleached states. A constant current density of 0.25 mA/cm^2 was applied for 40 s to color and bleach the films as this ensured the same concentration of the intercalated and deintercalated species (10 mC/cm^2) in all the films. Optical measurements were performed on as-deposited and annealed films. The open circuit memory of the films was not very good, i.e., the bleached state of the films was not retained over a period long enough to carry the measurements accurately for determining the coloration efficiency values.

3. Results and discussion

The PB has polyelectrochromic feature with four redox states – the colorless Everitt's salt (ES), deep blue PB, Berlin green (BG) and Prussian yellow (PY) in sequence from most reduced to most oxidized state [11]. Amongst these four redox states, the PB/ES redox system is the most stable and the reversible couple. The possibility of going reversibly between colored PB and colorless ES leads to anodic electrochromism. The PB insoluble form supports a redox reaction as follows:

$$\underset{\text{PB(blue)}}{Fe_4{}^{3+}[Fe^{II}(CN)_6]_3} + xM^+ + xe^- \leftrightarrow \underset{\text{ES(transparent)}}{M_x{}^+Fe_x{}^{2+}Fe^{3+}_{4-x}[Fe^{II}(CN)_6]_3} \quad (1)$$

where M^+ is the cation such as K^+, Li^+ or H^+, etc., and this makes PB a pivotal inorganic non-oxide electrochromic material [10,12–15].

The PB is a classical mixed valence compound with two forms known as insoluble and soluble PB with the respective chemical formulae as $Fe_4{}^{III}$ $[Fe^{II}$ $(CN)_6]_3$ and $KFe^{III}Fe^{II}(CN)_6$, distinguished by the presence or absence of potassium. The idealized basic structure of PB, with a completely ordered unit cell, is shown to be face centered cubic with $\rightarrow Fe^{II} \leftarrow C{\equiv}N \rightarrow Fe^{III} \leftarrow N{\equiv}C \rightarrow Fe^{II} \leftarrow$ linkages along all three crystallographic directions creating an open framework, with all metal ions in octahedral sites [16,17] According to detailed studies on PB [18] and related materials the structure is disordered, with one fourth of the ferrocyanide sites being unoccupied. The square openings in the cubic framework and the vacancies give PB a porous structure very much similar to that of zeolites conducive for insertion/extraction of ions rendering them suitable also as electrodes in rechargeable batteries. Due to bridging of the metal sites with the conjugated cyanide ligand, PB exhibits strong magnetic coupling and magnetic ordering. The cyanide ions bridge the high spin Fe^{III} and Fe^{II} ions so effectively that an intense charge transfer can occur resulting in a broad intense absorption band at 14000 cm^{-1}. Electrochemical redox reactions can also bring about such charge transfer interactions with concomitant color changes that are reversible as shown above by Eq. (1).

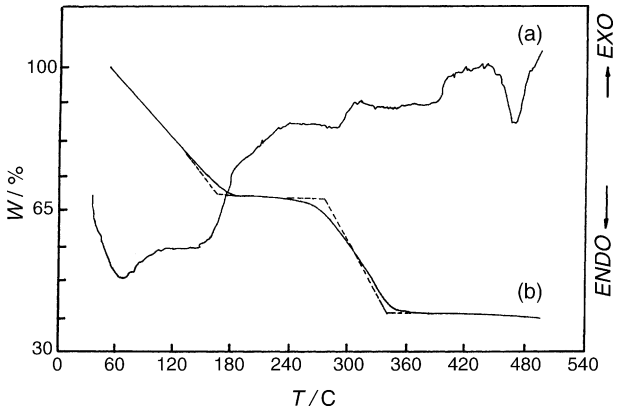

Fig. 1. DSC (a) and TGA (b) traces of solid PB (scraped from the substrate) from room temperature to 450 °C recorded at 10 °C/min.

Our galvanostatically as-deposited PB films are dark blue in color and are confirmed to be "insoluble" form of PB on the basis of EDX analysis, the atomic % of different elements being N → 25.72, O → 27.74, Fe → 0.54, Si → 12.14, Na → 1.89, Ca → 1.96, showing complete absence of K. These films showed high mechanical and chemical stability in the liquid electrolyte (1 M $LiClO_4$-PC). Annealing at temperatures up to 220 °C retained the blue color of the films but with decreased coloration density. Higher annealing temperature transformed the films to typical rust color.

XRD patterns for all the films, as-deposited and annealed, are completely devoid of any sharp diffraction peaks illustrating their amorphous structure.

Fig. 1 illustrates the DSC and TGA profiles of PB powder scraped from the as-deposited PB film. Two broad and intense endotherms are evident in the DSC profile respectively in the temperature ranges from room temperature to 100 °C and from 100 to 200 °C and these are followed by one prominent sharp endotherm at a higher temperature above 440 °C. Corresponding to the two endotherms at lower temperatures, there is a two step weight loss in the TGA profile, with an intermediate plateau in the temperature range 214–238 °C, amounting totally to about 50%, up to about 360 °C. These can be interpreted due to loss of uncoordinated and coordinated water present in PB [19,20]. The presence of the intermediate plateau can be inferred to be due to a stable phase with coordinated water molecules after loosing the uncoordinated water molecules at lower temperature. Highly hydrated nature of PB films is thus evident. Beyond 350 °C there is some weight loss but is insignificant in comparison to the weight loss at lower temperatures. There are two weak endotherms in the intermediate temperature range. These are explained in the relevant sections to follow.

In Fig. 2 are shown FTIR spectra of (a) as-deposited and films annealed respectively at (b) 100 °C, (c) 220 °C, (d) 350 °C, and (e) 500 °C and Table 1 gives the positions and intensities of the bands in these spectra along with their assignments. All the spectra can be divided into three main frequency

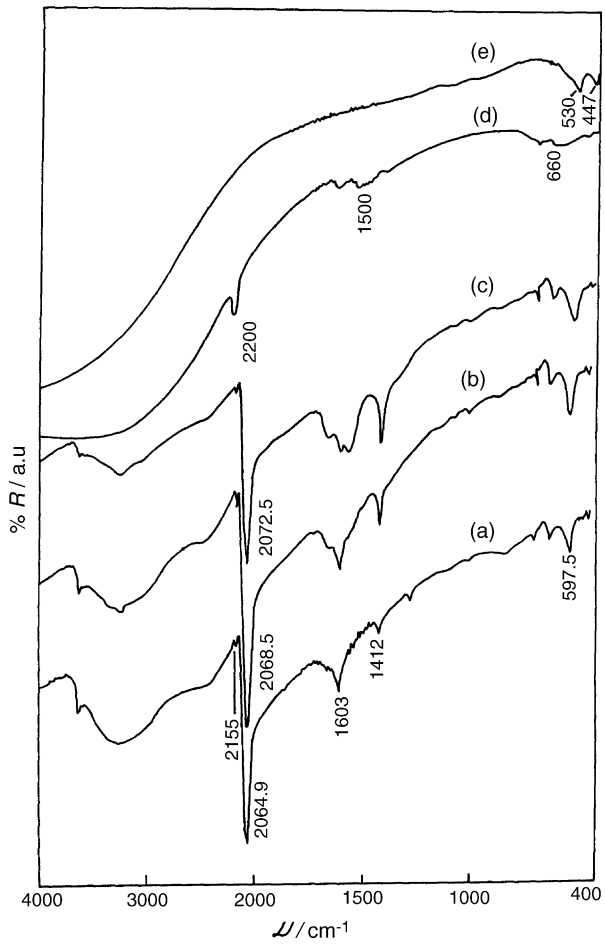

Fig. 2. FTIR spectra of PB films (a) as-deposited and annealed at (b) 100 °C, (c) 220 °C, (d) 350 °C, and (e) 500 °C.

regions (1) 4000–2500 cm^{-1}, (2) 2500–1400 cm^{-1}, and (3) 1000–400 cm^{-1}. It can be noticed that the spectra of the as-deposited and films annealed at 100 and 220 °C have many features that are similar.

In the high frequency region wherein the bands due to O–H stretching mode occur, there exists a very broad medium intensity band peaking at 3261 cm^{-1} along with a relatively sharp band on the high frequency side at 3623 cm^{-1} in the spectrum of the as-deposited PB film. These two bands can be attributed respectively due to stretching modes of bonded and free O–H groups [21]. With annealing (spectra b and c), these bands gradually decrease in intensity while they are completely absent for high temperature annealing. Both these observations corroborate loss of water as observed by thermal studies.

In the second frequency region the spectra a, b, and c, i.e., for as-deposited and films annealed at 100 and 220 °C respectively, each have the most intense and sharp band peaking respectively at 2064.9, 2068.5, and 2072 cm^{-1} and this band is accompanied on its higher frequency side by a very weak band at 2155 cm^{-1} invariant in position irrespective of the annealing treatment. A sharp ν (CN) band between 2200 and 2000 cm^{-1} identifies cyano complexes [22]. Upon coordination to a metal the ν (CN) shifts to frequencies higher than that for free CN^- which lies at 2080 cm^{-1} (aqueous solution). The upward shift of this mode is governed by (1) the electronegativity, (2) the oxidation state, and (3) the coordination number of the metal. Smaller electronegativity, lower oxidation state and increased coordination number decrease the ν (CN) value. Further, in bridged cyano complexes, the M–C≡N group forming a M–C≡N-M′ (M and M being the two metals which in the present case both are Fe ions with different oxidation states) type bridge, is reported [22] to shift ν (C≡N) to a higher and ν (MC) to a lower frequency. On the basis of these considerations and the observed upward shift of the lower frequency band with annealing, the lower frequency bands have been assigned to ν (CN) mode associated with Fe^{II} as against the high frequency band to ν (CN) mode associated

Table 1
Infrared band positions (cm^{-1}) for the as-deposited and annealed PB films

Serial number	As-deposited PB film	PB films annealed at				Assignment
		100 °C	220 °C	350 °C	500 °C	
1	3623 (m)	3623 (m)	3623 (m)	–	–	ν (OH), free OH
2	3261 (m,b)	3261 (m,b)	3261 (m,b)	–	–	ν (OH), bonded OH
3	–	–	–	2200	–	ν_{as} (C≡N), (NCO)
4	2155 (vw)	2155 (vw)	2155 (vw)	–	–	ν (C≡N), (Fe^{3+})
5	2064.9 (vs, sharp)	2068.5 (vs, sharp)	2072.5 (vs, sharp)	–	–	ν (C≡N), (Fe^{2+})
6	–	1650 (w)	1665 (mw)	–	–	δ (HOH)
7	1603 (m)	1603 (m)	1603 (m)	1603 (m)	–	δ (HOH)/ν C=O
8	–	–	1565 (m)	–	–	
9	–	–	–	1500	–	
10	1412 (w)	1412 (m)	1412 (m)	–	–	δ (OH)
11	–	–	–	1285	–	ν_s (NCO), cyanato complex
12	–	–	–	660	–	δ (NCO) cyanato complex
13					600 (sh)	
14	597.5 (m)	597.5 (m)	597.5 (m)		–	ν (Fe–C), cyano complex
15	–	–	–	–	530	ν (Fe–O) Fe_2O_3
16	499.2 (w)	499.2 (w)	499.2 (w)	–	–	δ (Fe–C–N) cyano complex
17	–	–	–	451	447	ν (Fe–O) Fe_2O_3

m: medium, b: broad, vs: very strong, vw: very weak, w: weak.

with Fe^{III}. On annealing at 100 and 220 °C, the lower frequency band shows an upward shift with simultaneous decrease in its intensity. These observed changes could be ascribed to presence of Fe with increased oxidation state and decrease in the contribution associated with Fe^{II}. In other words, this points towards gradual change of Fe^{II} to Fe^{III}.

When annealed at higher temperature the color of the film changes to rust and there is only one band at 2200 cm^{-1} for the films annealed at 350 °C (Fig. 2(d)) and for the film annealed at 500 °C (Fig. 2(e)) it no more exists. These are the manifestations of conversion of PB to Fe_2O_3 through an intermediate phase attributable to "cyanato complex" [22] and can thus be correlated to higher temperature endothermic peaks observed in the DSC pattern.

Majority of the cyanato complexes which are N bonded (M–NCO) rather than oxygen bonded (M–OCN) have three characteristic vibrations consisting mainly of vibrational modes of CN and CO groups. The reported frequencies for $[Fe(NCO)_4]^{2-}$ are ν (C≡N) at 2182 cm^{-1}, ν (C–O) at 1337 cm^{-1} and δ NCO at 619 cm^{-1} [23,24]. In the bridged cyanato complexes, as in bridged cyano complexes discussed above, the former band shifts to higher and the latter two to lower frequencies. Accordingly, the weak bands at 2200, 1285 and 660 cm^{-1} in the spectrum (Fig. 2(d)) of the PB film annealed at 350 °C have been assigned respectively to ν (C≡N), ν (C–O) and δ NCO of the bridged cyanato complex formed at this temperature.

In the intermediate frequency region, there are two or more bands of medium intensity in the spectra of the films annealed at 100 and 220 °C at around 1660 and 1412 cm^{-1}, which no more appear in the spectra of the films annealed at 350 and 500 °C. Their positions correspond to in plane bending modes δ (HOH) and δ (OH), due to hydrated and hydroxylated nature of the films.

In addition to ν (CN), the cyano complexes exhibit ν (MC), δ (MCN) and δ (CMC) bands in the low frequency region. Assignment of these modes made on the basis of normal coordinate analysis for various hexacyano complexes indicate them to lie in the regions 600–350, 500–350, and 130–60 cm^{-1}, respectively. Consistent with this, the bands at around 597.5 and 499.2 cm^{-1} in the spectra (a, b and c) have been assigned respectively to the ν (FeC), δ (FeCN) modes. In the spectrum for the film annealed at 350 °C (d) there is a broad band peaking at 660 cm^{-1}. This is due to δ NCO mode of the bridged cyanato complex.

Further increase of annealing temperature to 500 °C has resulted in two very weak bands at 530 cm^{-1}, 447 cm^{-1} along with a shoulder at 600 cm^{-1} (e). The positions of these two bands are comparable to those (555 and 459 cm^{-1}) corresponding to α-Fe_2O_3 evolved via the partial conversion of β-FeOOH to α-Fe_2O_3 [25,26] and to (520 and 432 cm^{-1}) in the sol–gel derived Fe_2O_3 films by Orel et al. [27]. In view of the influence of various factors such as the degree of crystallinity, morphology of the particles and the aggregation and matrix effects on the spectrum of α-Fe_2O_3, the bands in the spectrum of the PB film heated at 500 °C have been assigned to Fe–O stretching vibrations. The deviation of the spectrum from the usual shape recorded for crystalline samples of α-Fe_2O_3 was thought to be because of the amorphous nature of the phase formed. Indeed, our XRD investigations confirmed this speculation by giving a broad hump in the low 2θ region of the XRD pattern.

Thus, the FTIR investigations have clearly revealed the evolution of α-Fe_2O_3 on annealing PB films: loosing water at lower temperatures, transforming into a cyanato complex and subsequently converting to α-Fe_2O_3. The formation of α-Fe_2O_3 was also confirmed by the analysis carried out for the scraped material from the PB film heat treated at 500 °C by flame atomic absorption as well as the XPS investigations.

Though the films appeared quite homogeneous and smooth to the naked eye, under the scanning electron microscope, the morphology of the films was found to be temperature-dependent. Fig. 3 illustrates the micrographs of the as-deposited and the annealed films with the same magnification factor. As is evident, cracks appear to be an inherent feature irrespective of the annealing temperature. The surface of the as-deposited films, though appears quite homogeneous, it has very fine cracks. However, these cracks have no effect on their electrochromic performance. The cracks appear to have same width over the complete surface of the film annealed at a particular temperature. However, heat treatment seems to have resulted in widening the cracks and in addition there appear some small white spots that are randomly distributed, the volume fraction of which is seen to increase as a function of temperature of heat treatment. According to EDX analysis, these spots contain less amount of Fe than the other parts of the film.

Cracked but relatively smooth surface covered by a large amount of small clots for as-deposited PB films has been reported previously by Zadronecki et al. [28]. For PB films deposited on platinum and gold substrates which appeared homogeneous to the eye the SEM studies by Ellis et al. [29] revealed a structure typical of an organic sol having small particles with tendency to cluster. As much as one-fourth of the substrate was estimated to be void of PB. A lot of open structure with cracks and pores for electrodeposited films have also been observed by Chen and Ho and Feldman and Murray [30,31]. Based on our earlier TEM investigations [32] on as-deposited PB films the observed white spots may be explained as due to agglomerates and evaporation of large amount of water causing stresses in the films may be considered to be responsible for the generation of the cracks, which grow with annealing treatment at temperatures up to 220 °C. At higher temperature annealing, formation of more agglomerates and apparent lateral shrinkage of the film appears to manifest in larger cracks and more number of spots.

Our systematic XPS investigations carried out on as-deposited and annealed PB films have revealed the annealing treatment induced compositional changes along with important information supporting the SEM observations. Fig. 4 shows the deconvoluted XPS core-level spectra in the binding energy range 705–730 eV, obtained for as-deposited film and those annealed at 220 °C and 500 °C. The as-deposited film shows the spin–orbit splitting of the of the Fe 2p level, manifested as $Fe2p_{3/2}$ and $Fe2p_{1/2}$. However, deconvoluting the peaks into Gaussian components using appropriate positions and FWHM, shows that Fe exists in both Fe^{II} (708.5, 711 eV) and Fe^{III} (721, 724.3 eV) states. There is also a small component of $Sn2p_{3/2}$, (∼ 717 eV)

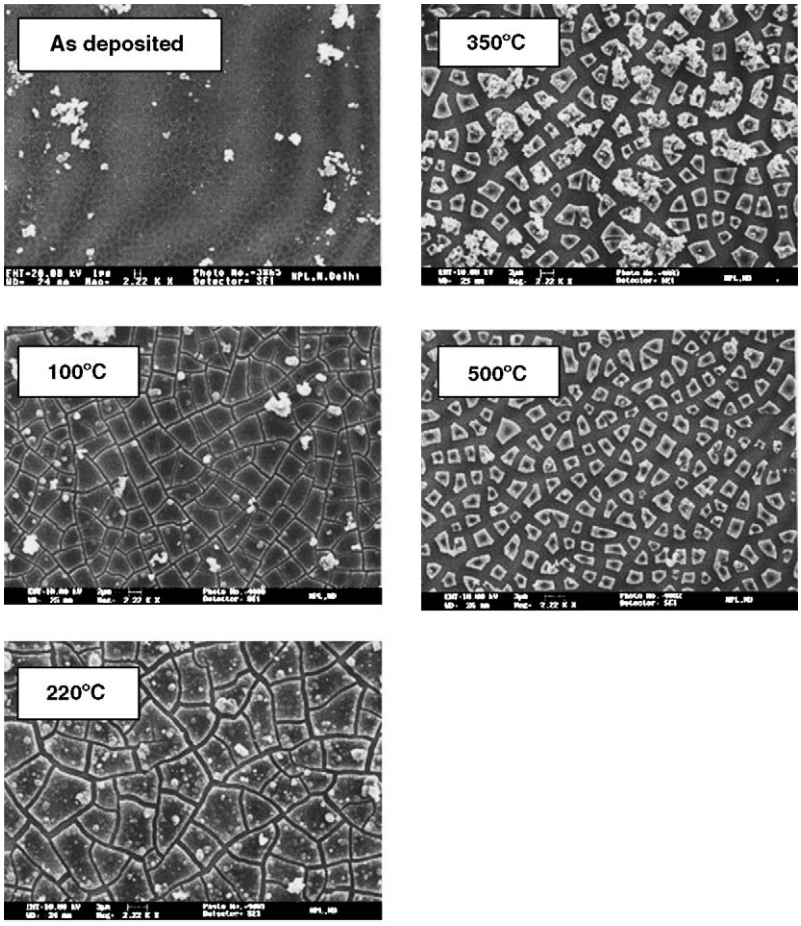

Fig. 3. Scanning electron micrographs of as-deposited PB film and PB films annealed at different temperatures.

which originates from the SnO_2 coated substrate. When the PB film is annealed at 220 °C, there is a clear shift in the $Fe2p_{3/2}$ from 708.5 to 711 eV. In fact, the Fe^{II} signature at 708.5 eV has completely disappeared, while the Fe^{III} signature at 711 eV has become very strong when annealed at higher temperatures. This suggests that the Fe^{II} have converted into Fe^{III} state, transforming to Fe_2O_3. It is also interesting to note a sharp increase of the intensity of the 717 eV peak, related to the $Sn3p_{3/2}$. Annealing at 500 °C enhances this transformation and the change to Fe_2O_3 phase is again clearly manifested. The increase in $Sn3p_{3/2}$ signal suggests that the substrate is being increasingly exposed with higher annealing temperatures. This corroborates the SEM results described earlier, resulting in 'cracking' up of the film due to loss of water component of the film. However, the XPS results give the additional information on the chemical state of Fe, which suggest the change from Fe^{II} to Fe^{III}. It is interesting to observe that the change is complete at 220 °C itself, and further annealing only increases the cracking of the sample.

One interesting feature remains puzzling. The relative intensity of $Fe2p_{3/2}$ and $Fe2p_{1/2}$ before and after annealing is striking. The $Fe2p_{1/2}$ peak is usually smaller than the $Fe2p_{3/2}$ in both the Fe and Fe_2O_3 standard samples. The fact that the $Fe2p_{1/2}$ is significantly stronger than $Fe2p_{3/2}$ is interesting, in the as-deposited case, where we have predicted a dominant Fe^{II} state. After annealing to higher temperatures this anomaly disappears and attains the standard values. The branching ratio of this spin–orbit states has been seen to differ significantly between atoms bonded at different sites [33]. This needs to be probed intensely to understand the role it plays in this system, and will be the focus of future work.

Though Fig. 4 shows only core-level spectra at the representative annealing temperatures, the experiments have been performed at different annealing temperatures. The results of the XPS studies and consequent deconvolution into Gaussian components are consolidated in Fig. 5. This figure consists of the change in the ratio of the $Fe2p_{3/2}$ peak in the Fe^{II} state and that in Fe^{III} state. The ratio shows continuous decrease with temperature. However, the decrease is much smaller up to 100 °C whereas there is a sharp decrease between 100–220 °C. At annealing temperature of 220 °C, where the complete desorption of water takes place from the film, the Fe^{II} state is completely quenched and transformation to Fe_2O_3 is complete. The curve on the alternate *y*-axis shows the ratio of $Sn3p_{3/2}$ to the $Fe2p_{3/2}$, and indicates the relative quantities of Sn and Fe as annealing proceeds. The curve shows clearly that the cracking process exposes the surface of the substrate linearly up to about 220 °C and then slightly slows down for higher annealing temperatures indicating the difference in the role of two different temperature regions.

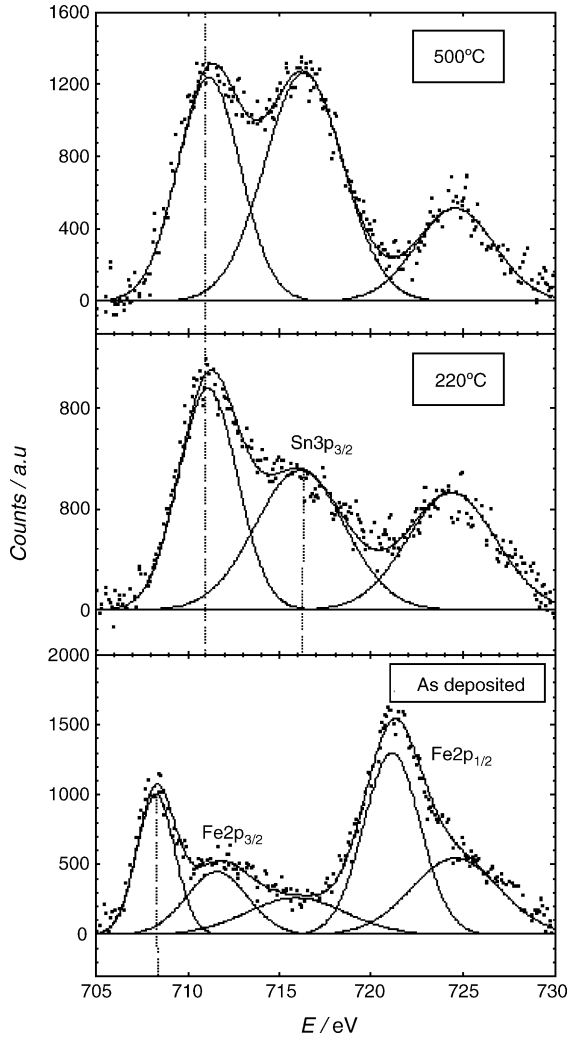

Fig. 4. XPS patterns of (a) as-deposited PB film and PB films annealed at (b) 220 °C, and (c) 500 °C.

As-deposited blue PB films after annealing treatment up to 220 °C retained their blue color but at higher temperatures the films showed typical rust color. These changes in the color of the films are reflected in their absorption spectra as shown in Fig. 6. As can be seen from this figure, the as-deposited PB

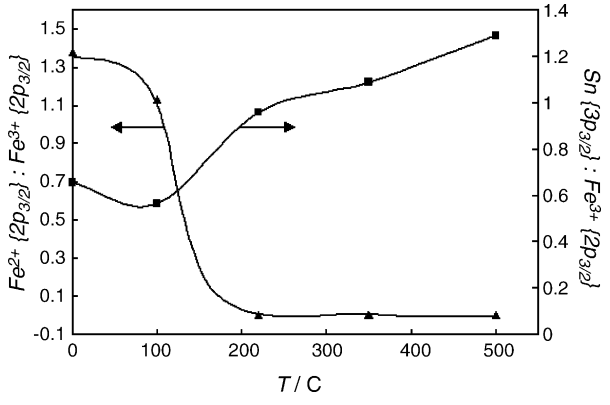

Fig. 5. Plot of Fe^{II}/Fe^{III} ($2P_{3/2}$) and Sn/Fe ratio as a function of annealing temperature.

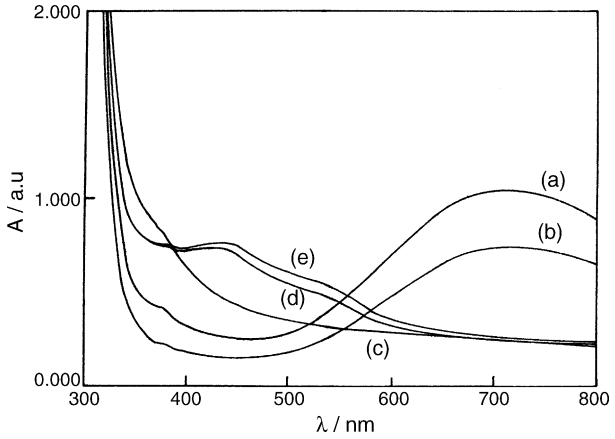

Fig. 6. Absorption spectra of PB films (a) as-deposited and annealed at (b) 100 °C, (c) 220 °C, (d) 350 °C, and (e) 500 °C.

film shows the characteristic broad absorption peak with its maximum at around 697 nm (14347 cm^{-1}). This corresponds to charge transfer between Fe^{III} to Fe^{II} ions. There is a progressive decrease in the intensity of this peak with annealing temperature and can be correlated to loss of water, as evidenced by the thermal, FTIR and XPS studies above, effectively decreasing the possible number of such transitions. The films annealed at and above 350 °C exhibit different characteristics with a weak peak between 400–450 nm and a shoulder at higher wavelength around 550 nm. Gatierrez and Beden [34] have assigned the peaks in these wavelength regions as due to iron oxide.

Coloration efficiencies determined by injecting a constant charge in the as-deposited PB film and are plotted (Fig. 7) as a function of wavelength in the $350 \leq \lambda \leq 850$ nm range. Coloration efficiency (η) at a particular wavelength correlates the optical density with charges intercalated per unit electrode area and can be expressed as

$$\eta(\lambda) = \frac{\Delta OD(\lambda)}{(q/A)} = \frac{\log(T_b/T_c)}{(q/A)} \quad (2)$$

where T_b and T_c are the transmittance of the film in the bleached and colored states, respectively. Coloration efficiency increases

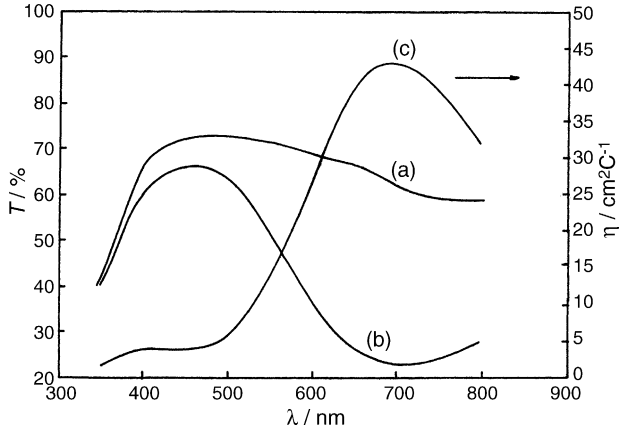

Fig. 7. Transmission spectra of PB film (a) bleached, (b) colored states, and (c) coloration efficiency under a constant current density of 0.25 mA/cm^2 applied for 40 s, between 300 and 800 nm.

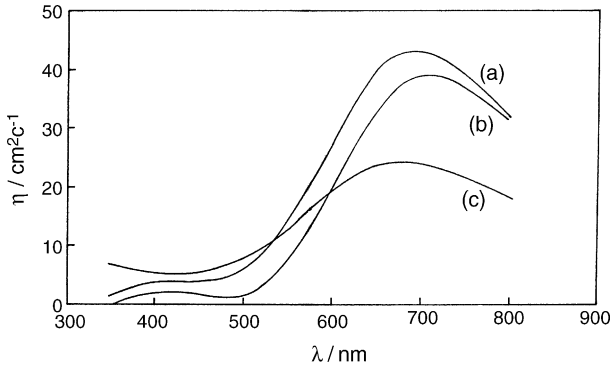

Fig. 8. Coloration efficiency as a function of wavelength of PB films (a) as-deposited and annealed at (b) 100 °C, and (c) 220 °C.

steadily as the wavelength is increased from 450 to 630 nm attaining its highest value of 42.8 cm^2/C at 700 nm. Although it decreases at higher wavelengths the value is still reasonably high, above 32 cm^2/C. Thus (a)WO_3–PB-based complimentary electrochromic window can make an effective control not only of the visible light, but also of the heat radiation. The data in Fig. 7 also indicates optical modulation variation with wavelength. Such a film when used as an active counter electrode in conjunction with a WO_3 film in an electrochromic device adds to overall coloration efficiency.

The coloration efficiency of the films annealed at temperatures up to 220 °C follow a similar trend in respect of their variation as a function of wavelength, as exhibited by the as-deposited films (Fig. 8). However, the maximum attainable coloration efficiency decreases with temperature with the values of 38.8 and 23.7 cm^2/C, respectively for the films annealed at 100 and 220 °C. It is noteworthy that the decrease in the value of coloration efficiency of the films annealed at 100 °C is far too less (9.3%) than that of the films annealed at 220 °C (44%). Similar result, of very little effect on the electrochemical behavior on the zeolitic or uncoordinated water, on PB as a positive electrode of lithium secondary battery, has been reported by Imanishi et al. [35].

The films were colored using a step potential in order to determine their ion storage capacities (ISC) or charges inter/deintercalated per unit active film area. and to ascertain the reversibility of the redox reactions bringing about coloration and bleaching. Coloration–bleaching characteristics of all the films at 632.8 nm are illustrated in Fig. 9 and in Table 2 are listed the coloration–bleaching times (t_c and t_b), coloration–bleaching charges (Q_c and Q_b) and ion storage capacities of the films. Coloration kinetics is observed to be faster than bleaching kinetics for all the films. The as-deposited films, as seen in the figure,

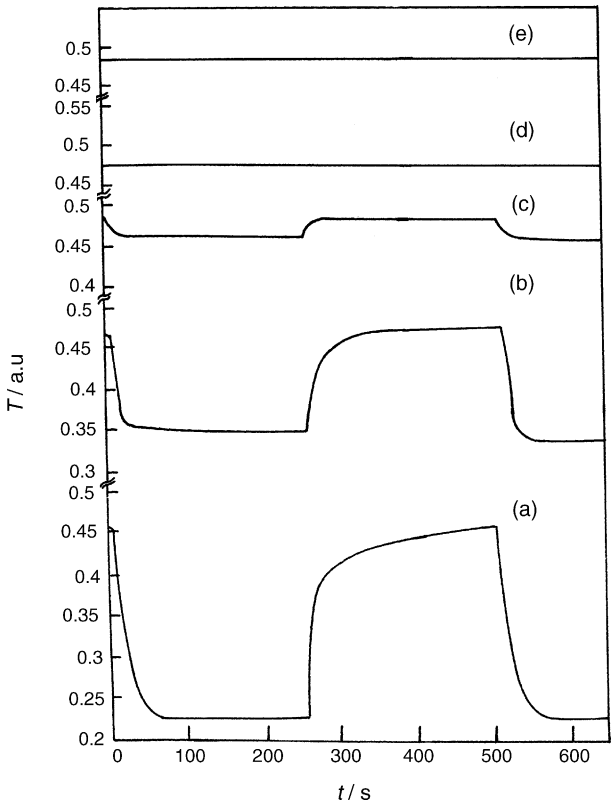

Fig. 9. Coloration–bleaching characteristics of PB films (a) as-deposited and annealed at (b) 100 °C, (c) 220 °C, (d) 350 °C, and (e) 500 °C, at 632.8 nm under an input square wave potential of ± 1 V at a frequency of 0.0016 Hz.

show an appreciable transmission modulation and subsequent annealing treatments up to 220 °C follow the decreasing trend in the modulation consistent with the transmission data (Fig. 6). On further heating at and above 350 °C, the films in addition to changing their color from blue to rust are seen to loose their electrochromic activity with no measurable optical modulation within the limits of accuracy for the measurements with our set-up. The switching times, ion storage capacity as well as the charges inter/deintercalated are seen to decrease with temperature. All the films exhibit excellent reversibility irrespective of the annealing treatment, as is evident from the values of Q_c and Q_b.

The decreased optical modulation on annealing is a clear evidence of decreased charge transfer interactions between Fe^{II} and Fe^{III} responsible for EC activity and is supported by the XPS results. It can thus very well be realized from the above results that whether coordinated or uncoordinated, the water present in PB films has profound effect on their electrochromic activity. The desorption of water in two steps as evident from TGA

Table 2
Coloration–bleaching times, charges and ion storage capacities of as-deposited and annealed PB films

Annealing temp (°C)	Coloration time t_c (s)	Bleaching time t_b (s)	Coloration charge Q_c (Col.)	Bleaching charge Q_b (Col.)	Ion storage capacity (mC/cm^2)	Coloration efficiency (cm^2/C)	Diffusion coefficient $D_a \times 10^{-11}$ cm^2/s
25 as-deposited	32	70	0.075	0.080	18	42.8	6.2
100	15	70	0.050	0.055	12	38.8	5.8
220	14	19	0.040	0.045	10	23.7	1.1

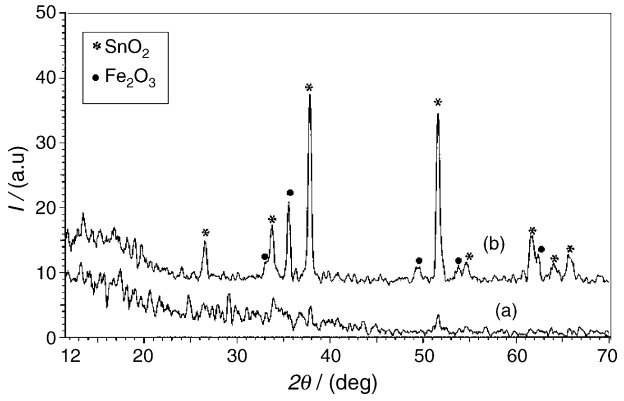

Fig. 10. XRD patterns of PB films (a) as-deposited (b) annealed at 500 °C for 10 h.

results is consistent with the decrease of electrochromic activity – the electrochemical redox reactions as in Eq. (1) above. It is noteworthy that consistent with the changes in the coloration efficiency, the electrochromic performance of the films is affected to a lesser degree for annealing treatment at 100 °C whereas these changes are magnified by a large extent for annealing at 220 °C. The sustained electrochromic activity but to less extent for films annealed at 100 and 220 °C and its disappearance for the films annealed at 350 °C has direct correlation with the water content in the film bound in different manner. Insoluble form of PB which is characterized by interstitial hydrated Fe^{III} [36], on loosing water with concomitant loss of electrochromic activity is bound to restructure the film. The neutron diffraction studies by Herren et al. [4] have shown that the dehydration of polycrystalline bulk PB sample leaves its iron-cyanide network intact giving microporous solids. The water free sample as shown by these authors is still cubic face centered but with a slightly contracted cell compared to the hydrated compound. The $Fe(CN)_6$ octahedra in the water free samples were shown to be distorted. The distortion was shown to be equivalent to deviation of the Fe–C–N–Fe arrangement from linearity. In contrast to the bulk polycrystalline PB sample of these authors since our highly electrochromically active films were XRD amorphous (Fig. 10(a)) no direct information either about the possible changes in the linear Fe–C–N–Fe arrangement or the size of the interstitial openings that allow inter/deintercalation of the Li ions responsible for electrochromic activity could be obtained. The films even after annealing at the highest temperature (500 °C) for duration of 15 min remained XRD amorphous. Identification of the phase/composition of the PB films annealed at 500 °C which were amorphous to X-rays was possible when these film were subjected to the annealing treatment at the same temperature for extended duration. When annealed for 10 h these films showed the XRD pattern as illustrated in Fig. 10(b) giving strong and sharp bands that could be indexed to a hexagonal Fe_2O_3 phase according to ICDD PDF file no 33–664. This supports the findings of the atomic absorption, FTIR and XPS studies discussed above.

Typical cyclic voltammograms in the 10th cycle recorded at a scan speed of 20 mV/s for all films under investigation are displayed in Fig. 11. The voltammogram profile (Fig. 11(a)) for the as-deposited film matches well with the reported CV plots [5,12,13] of PB films deposited similarly. PB films on platinum substrate show zero separation of voltammetric peaks [37] for the reduction to Everrit's salt and reoxidation. In contrast, the PB films under investigations exhibit a definite separation of few mV. This is attributable to the resistivity of the FTO substrate layer. The films were subjected to repeated reduction and oxidation over a large number of cycles and were found to be characterized by excellent reproducible response over 10,000 cycles at room temperature indicating a large number of switchings without great degradation or irreversible side reactions. The sustained, high overall coloration efficiency of the films suggests the insertion/extraction of Li ions into and out of the as-deposited PB films.

A series of cyclic voltammograms were recorded at scan rates that varied between 1 and 50 mV/s. The dependence of the peak currents on the square root of the scan rate implied the electrode kinetics being influenced by the diffusion of Li^+ ions into the surface bound iron hexacyanoferrate for the PB → ES redox couple. The diffusion coefficients have been calculated using the Randles–Servcik equation

$$I_p = 2.72 \times 10^5 \times n^{3/2} \times D^{1/2} \times C_0 \times v^{1/2}$$

where the diffusion coefficient D is in cm^2/s, the concentration of the active ion in solution C_0 the concentration of Li^+ in the liquid electrolyte and is in mol cm^3, the sweep rate v is in volt/s, the number of electrons n is 1 and the peak current density I_p is in A/cm^2. The calculated values of D for the cathodic and anodic cycles, respectively are $D_c = 6.9 \times 10^{-11}$ and $D_a = 6.2 \times 10^{-11}$ cm^2/s. Exhaustive literature available on the electrochemical behavior of PB films in aqueous/acetonitrile media containing alkali metal ions as supporting electrolyte cations have shown similar comparable values of D during oxidation and reduction, as in the present studies, lying generally in the range 10^{-9}–10^{-10} cm^2/s [13,17,38–45]. However, relevant studies in non-aqueous media, though important for applications of PB films in electrochromic devices, are meager. The low values of $D \sim 10^{-11}$ cm^2/s in the present studies can be attributed as due to the supporting electrolyte based on propylene carbonate.

The films annealed at 100 °C demonstrated voltammogram (Fig. 11(b)) very much similar to that shown by the as-deposited films. However, the peak current density for the cathodic as well as anodic cycle has decreased by a small amount. The cyclic durability was almost invariant. Both these films demonstrated excellent reversibility, the ratio of the charges inter and deintercalated during the bleaching and coloring cycles never being less than 0.9 and for majority of the cycles being 1. The shape of the voltammogram for the film annealed at 220 °C has exhibited some change in its shape along with a drastic change in the peak current density values. These changes that are in accordance with the changes observed in coloration efficiency and ion storage capacity once again evidence very less effect in the electrochromic and electrochemical performance of PB films by annealing at 100 °C. In contrast, annealing at 220 °C decreases the electrochromic efficiency in a major way, although the films still retain their blue color.

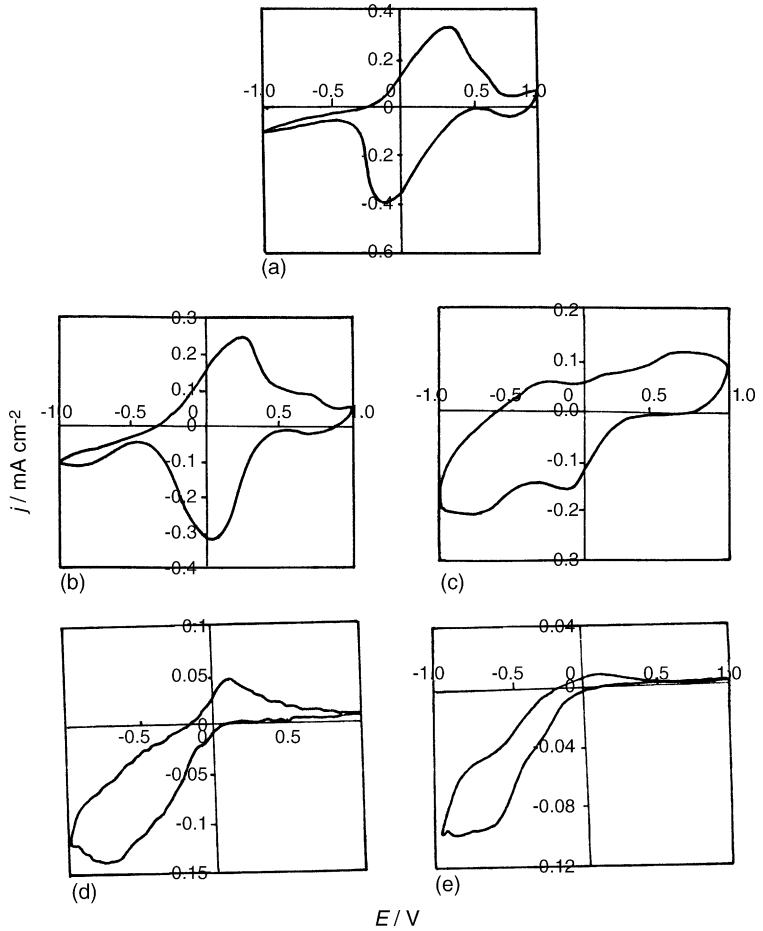

Fig. 11. Cyclic voltammograms of PB films (a) as-deposited annealed at (b) 100 °C, (c) 220 °C, (d) 350 °C, and (e) 500 °C at a scan speed of 20 mV/s in a 1 M $LiClO_4$-PC electrolyte.

Annealing at temperatures above 220 °C, the shapes of the voltammograms are much different than the ones observed for the films annealed at lower temperatures. The voltammogram (Fig. 11(d)) for the film annealed at temperature 350 °C has unusual shape while the one for the films annealed at 500 °C (Fig. 11(e)) is similar to that reported by Orel [27] for the sol–gel deposited iron oxide films. With cycling these films exhibited continuously decreasing peak current density values demonstrating very poor durability – their voltammogram shrinking in each subsequent cycle – with the current attaining almost a negligible value. As judged by the naked eye, the rust color of the films became lighter with cycling. Both the reversibility and durability of the films are affected adversely. These films exhibited decreasing electrochemical activity in successive cycles, their original rust color fading with cycling. These observations could be correlated to gradual dissolution of the film on cycling. The rate of electrochemical reductive dissolution was investigated by Grygar [46–48] for various modifications of ferrihydrite, FeOOH and Fe_2O_3. The rate of electrochemical dissolution was shown by these authors to be phase-specific in a manner very similar to their reactivity toward chemical reductive dissolution. The influence of the distribution function of the particle size was demonstrated to influence the peak current in voltammetry.

A glance at the values of the diffusion coefficients in Table 2 illustrates that it decreases with annealing temperature following a trend as that of the other performance characteristics of the films. The rate of diffusion of lithium ions which is highly sensitive to the microstructure of the films is thus proved to be highly dependent on the water content in the films.

4. Conclusions

Prussian blue (PB) films were deposited galvanostatically on transparent conducting coated glass plates. Films as-deposited and subjected to annealing treatment at different temperatures up to 500 °C, were characterized for their morphological (SEM), thermal (TGA/DSC), structural (XRD, FTIR), compositional (XPS), and electrochromic properties. The as-deposited films are highly hydrated, amorphous and with fine cracked surface. The films retain their amorphicity irrespective of the annealing temperature. The desorption of coordinated and non-coordinated water that takes place in two steps up to 220 °C results in degradation of the electrochromic performance of the films in terms of switching times, coloration efficiency, ion storage capacity, diffusion coefficient and enhancement of the cracks. These changes are accompanied by transformation of

Fe^{II} to Fe^{III} without affecting significantly the reversibility of the redox reaction responsible for coloration–bleaching. Importantly, the changes in the coloration efficiency are far too less for the films annealed at 100 °C as compared to the films annealed at 220 °C. This is advantageous for fabricating electrochromic devices by methods that demand heating up to 100 °C, without affecting the performance significantly. Annealing at higher temperatures results in enhanced transformation of Fe^{II} to Fe^{III} yielding α-Fe_2O_3, via an intermediate cyanato complex phase, rendering its typical rust color to the films and further enhancing the cracks. Cyclic voltammetry demonstrates feeble and short-lived electrochromism of the high temperature annealed films.

Acknowledgements

Financial support from the Ministry of Non-Conventional Energy Source (MNES) is gratefully acknowledged. The authors thank Dr. D. Gupta for recording FTIR spectra, Dr. Nahar Singh for carrying out atomic absorption measurements and Ms. Swati Gupta for helping in the experimental work.

References

[1] C.G. Granqvist, Handbook of Inorganic Electrochromic Materials, Elsevier, New York, 1995.
[2] S.K. Deb, Sol. Energy Mater. Sol. Cells 25 (1993) 327.
[3] C.M. Lampert, Sol. Energy Mater. Sol. Cells 52 (1998) 207.
[4] F. Herren, P. Fischer, A. Ludi, W. Halg, Inorg. Chem. 19 (1980) 956.
[5] M.A. Habib, S.P. Maheshwari, M.K. Carpenter, J. Appl. Electrochem. 21 (1991) 203.
[6] K.C. Ho, T.G. Rukavina, C.B. Greenberg, J. Electrochem. Soc. 141 (1994) 2061.
[7] K.C. Ho, Electrochim. Acta 44 (1999) 3227.
[8] L.C. Chen, K.C. Ho, Electrochim. Acta 46 (2001) 2151.
[9] L. Su, H. Wang, Z. Lu, Mater. Chem. Phys. 56 (1998) 266.
[10] K.H. Heckner, A. Kraft, Solid State Ionics 152–153 (2002) 899.
[11] P.M.S. Monk, R.J. Mortimer, D.R. Rosseinsky, Electrochromism Fundamentals and Applications, published jointly by VCH Verlagsgesellschaft mbH, Weinheim (FRG) and VCH Publishers Inc., New York NY (USA), 1995, p. 101 (Chapter 6).
[12] M.A. Habib, S.P. Maheshwari, J. Electrochem. Soc. 23 (1993) 44.
[13] K. Itaya, K. Shibayama, S. Toshima, J. Appl. Phys. 53 (1982) 804.
[14] D.W. De Berry, A. Vinhbeit, J. Electrochem. Soc. 130 (1983) 249.
[15] A. Kraft, M. Rottmann, K.H. Heckner, Sol. Energy Mater. Sol. Cells, in press.
[16] S.M. Girolami, J. Am. Chem. Soc. 121 (1999) 5593.
[17] K. Itaya, N. Shoji, I. Uchida, J. Am. Chem. Soc. 106 (1984) 3423.
[18] H.J. Buser, D. Schwarzenbach, W. Petter, A. Ludi, Inorg. Chem. 16 (1977) 2704.
[19] B. Bal, S. Ganguli, M. Bhattacharrya, J. Phys. Chem. 88 (1984) 4575.
[20] S. Ganguli, M. Bhattacharrya, J. Chem. Soc. Faraday Trans. 1, 79 (1983) 1513.
[21] Chemical Applications of Infrared Spectroscopy, C.N.R. Rao Academic Press, 1963, p. 175.
[22] K. Nakamoto, Infrared and Raman Spectra of Inorganic and Coordination Compounds, Wiley-Interscience Publication, John Wiley & Sons, New York, 1978, p. 259.
[23] D. Forster, D.M.L. Goodgame, J. Chem. Soc. 262 (1965).
[24] A.R. Chugtai, R.N. Kelkar, J. Inorg. Nucl. Chem. 31 (1969) 633.
[25] S. Music, G.P. Santana, G. Smit, V.K. Garg, J. Alloy. Compd. 278 (1998) 291.
[26] A. Saric, S. Music, K. Nomura, S. Popovic, J. Mol. Struct. 480–481 (1999) 633.
[27] B. Orel, M. Macek, F. Svegl, Thin Solid Films 246 (1994) 131.
[28] H.M. Zadronecki, P.K. Wrona, Z. Galus, J. Electrochem. Soc. 146 (1999) 620.
[29] D. Ellis, M. Eckhoff, V.D. Neff, J. Phys. Chem. 85 (1981) 1225.
[30] L.C. Chen, K.C. Ho, J. Electrochem. Soc. 149 (2002) E40.
[31] B.J. Feldman, R.W. Murray, Inorg. Chem. 26 (1987) 1702.
[32] A.K. Srivastava, R. Kishore, Swati, S.A. Agnihotry, Indian J. Eng. Mater. Sci. 11 (2004) 315.
[33] M.T. Seiger, T. Miller, T.C. Chiang, Phys. Rev. Lett. 75 (1995) 2043.
[34] C. Gatierrez, B. Beden, J. Electroanal. Chem. 293 (1990) 253.
[35] N. Imanishi, T. Morikawa, J. Kondo, Y. Takeda, O. Yamamoto, N. Kinugasa, T. Yamagishi, J. Power Sources 79 (1999) 215.
[36] R.E. Wilde, S.N. Ghosh, B.J. Marshall, Inorg. Chem. 9 (1970) 2512.
[37] K. Itaya, T. Ataka, S. Toshima, J. Am. Chem. Soc. 104 (1982) 4767.
[38] V.D. Neff, J. Electrochem. Soc. 132 (1985) 1382.
[39] D. Emis, M. Eckhott, V.D. Neff, Phys. Chem. 85 (1981) 1225.
[40] R. Messina, J. Penchon, J. Appl. Electrochem. 10 (1980) 655.
[41] D. Engel, E.W. Grabner, Ber. Bunsengers. Phys. Chem. 89 (1985) 982.
[42] P.J. Kulesza, K. Doblhofer, J. Electroanal. Chem. 274 (1989) 95.
[43] K. Ogura, M. Kaneko, J. Mol. Catal. 31 (1985) 49.
[44] G. Horanji, G. Inzelf, P.J. Kulesza, Electrochim Acta 35 (1990) 811.
[45] M. Jaylakshmi, H. Gomathi, G. Prabhakar Rao, Sol. Energy Mater. Sol. Cells 45 (1997) 201.
[46] T. Grygar, J. Electroanal. Chem. 405 (1996) 117.
[47] T. Grygar, J. Solid State Electrochem. 1 (1997) 77.
[48] T. Grygar, J. Solid State Electrochem. 2 (1998) 127.